Epithelial re-organization and dynamics of progression through mitosis in *Drosophila* separase complex mutants

Rahul Pandey, Stefan Heidmann and Christian F. Lehner*

BZMB, Department of Genetics, University of Bayreuth, 95440 Bayreuth, Germany

*Author for correspondence (e-mail: chle@uni-bayreuth.de)

Accepted 24 November 2004
Journal of Cell Science 118, 733-742 Published by The Company of Biologists 2005
doi:10.1242/jcs.01663

Summary

Separase cleaves a subunit of the cohesin complex and thereby promotes sister chromatid separation during mitotic and meiotic divisions. *Drosophila* separase associates with regulatory subunits encoded by the *pimples* and *three rows* genes. Three rows and Pimples, the *Drosophila* securin, are required for sister chromatid separation during mitosis. Budding yeast separase provides other functions in addition to cohesin subunit cleavage, which are required for spindle organization and temporal regulation during exit from mitosis. Therefore, using time-lapse imaging in live embryos, we have carefully analyzed progression through mitosis in *pimples* and *three rows* mutants. We demonstrate that despite the total failure of sister chromatid separation, exit from mitosis, including a complete cytokinesis, proceeds with only a minor temporal delay in the epidermal cells of these mutants. Interestingly, however, pronounced defects in the epithelial organization develop in the following interphase, indicating that the separase complex is not only important for genetic stability but also and perhaps indirectly for epithelial integrity.

Supplementary material available online at
http://jcs.biologists.org/cgi/content/full/118/4/733/DC1

Key words: Cytokinesis, Centrosome, Junctional dynamics, Mitotic exit network (MEN), Cdc fourteen early anaphase release (FEAR), Separase

Introduction

Separase is a thiol protease that cleaves α-kleisin subunits (Scc1/Mcd1/Rad21/Rec8 family members) of cohesin complexes and thereby contributes to sister chromatid separation during mitotic and meiotic divisions (Buonomo et al., 2000; Uhlmann et al., 1999; Uhlmann et al., 2000). Before anaphase onset, protease activity is inhibited by securin, a protein that binds to separase during interphase. However, at the metaphase-to-anaphase transition securin is degraded after ubiquitination by the anaphase-promoting complex/cyclosome (APC/C) (Ciosk et al., 1998; Cohen-Fix et al., 1996; Funabiki et al., 1996; Uhlmann et al., 2000; Zou et al., 1999).

Apart from α-kleisin cleavage, budding yeast separase has been shown to function in an additional pathway during exit from mitosis (Stegmeier et al., 2002; Tinker-Kulberg and Morgan, 1999). Interestingly, protease activity does not appear to be required in this FEAR (Cdc fourteen early anaphase release) pathway. Catalytically inactive separase versions are sufficient to trigger Cdc14 release from the nucleolus during early anaphase (Sullivan and Uhlmann, 2003). The released active Cdc14 phosphatase promotes exit from mitosis (Jaspersen et al., 1999; Shou et al., 1999; Stegmeier et al., 2002; Visintin et al., 1998). The inner centromere protein Sli15 is dephosphorylated by Cdc14, resulting in the transfer of Sli15-Ipl1(Aurora) kinase complexes from a centromeric chromosomal localization to the central spindle (Pereira and Schiebel, 2003). Slk19, another yeast protein, which transfers to the central spindle during exit from mitosis, is also regulated by separase. Slk19 associates with separase following securin degradation. Slk19 and its cleavage by separase enhances the stability of anaphase spindles (Sullivan et al., 2001; Ross and Cohen-Fix, 2004). Moreover, Slk19 co-operates with separase in the early anaphase release of Cdc14. In addition to regulating spindle and mitotic exit dynamics, FEAR has recently been shown to promote sister chromatid separation in the nucleolus by stimulating the binding of condensin complexes to the rDNA region (D'Amours et al., 2004; Sullivan et al., 2004).

The FEAR pathway, however, does not appear to be absolutely essential. Completion of mitosis is only transiently delayed by about 30 minutes in separase mutants, but eventually cells exit from mitosis because Cdc14 release in budding yeast can also be triggered by an additional regulatory system, the mitotic exit network (MEN). In wild-type cells, MEN activation is controlled by the mitotic spindle position and it maintains Cdc14 activity after the initial release by FEAR (Bardin et al., 2000; Stegmeier et al., 2002).

It is not yet clear whether pathways comparable to budding yeast FEAR and MEN operate in higher eukaryotes that also express Cdc14 homologues. Some, but not all of the other pathway components can also be identified in higher eukaryotes, but it remains to be determined whether Cdc14 and the other apparent homologues provide the same function as in yeast. In particular, it is not known whether separase provides FEAR-like functions in higher eukaryotes. Cytokinesis and

Journal of Cell Science

Journal of Cell Science

exit from mitosis are not delayed after RNAi-mediated separase elimination in *C. elegans* (Siomos et al., 2001). In contrast, completion of cytokinesis appears to depend on separase function in human cells (Hauf et al., 2001; Waizenegger et al., 2000).

To elucidate the role of separase during completion of mitosis in further detail, we describe phenotypic analyses in *Drosophila*. During the evolution of *Drosophila*, the separase gene has apparently become two genes, *three rows* (*thr*) and *Separase* (*Sse*) which encode the N-terminal regulatory domain and the C-terminal protease domain, respectively (Jäger et al., 2001; Jäger et al., 2004). *Drosophila* securin is encoded by the *pimples* (*pim*) gene (Leismann et al., 2000; Stratmann and Lehner, 1996). SSE, THR and PIM form a trimeric complex during interphase. After degradation of PIM at the metaphase-to-anaphase transition, SSE promotes sister chromatid separation and also cleaves the associated THR subunit, a process that contributes to timely SSE inactivation (Herzig et al., 2002). We have previously shown that a loss of PIM, THR or SSE function results in a failure of sister chromatid separation during mitosis (D'Andrea et al., 1993; Jäger et al., 2001; Stratmann and Lehner, 1996). In addition, non-cleavable THR versions were shown to interfere with cellularization (Herzig et al., 2002), which corresponds to a modified form of cytokinesis converting the syncytial into the cellularized blastoderm during interphase of cycle 14.

Here, we describe time-lapse analyses of progression through mitosis in live *pim* and *thr* mutant embryos. These analyses indicate that *Drosophila* separase is primarily required for sister chromatid separation. Cytokinesis and exit from mitosis appear to be surprisingly normal in the mutants. Cleavage furrows do not revert because of the non-separated chromatin mass present in these mutants. Interestingly, however, we find that the epithelial organization is severely affected in these mutants.

Materials and Methods

Fly stocks

Fly stocks with the mutant alleles pim^1, thr^1, dup^{a1}, pbl^{7O} and pbl^{11D} have been described previously (Lehner, 1992; Stratmann and Lehner, 1996; Whittaker et al., 2000). A pim^1 dup^{a1} double mutant chromosome was obtained by meiotic recombination. The pim^1 *pbl* double mutant embryos were obtained by crossing males heterozygous for pim^1 and pbl^{7O} with females heterozygous for pim^1 and pbl^{11D}. We used blue balancer chromosomes, which allowed the distinction of homozygous mutant from sibling progeny derived from heterozygous parents by anti-β-galactosidase labeling. *G147* carries a gene trap insertion in *CG31363*, resulting in expression of a microtubule-binding GFP fusion protein (Morin et al., 2001). *Spider* carries a gene trap insertion in *gilgamesh*, resulting in expression of a GFP fusion protein marking the cell cortex (Morin et al., 2001). The *His2AvD-mRFP* transgene driving expression of histone H2AvD fused to mRFP1 (Campbell et al., 2002) was constructed analogously to the *His2AvD-GFP* transgene (Clarkson and Saint, 1999) and will be described in detail elsewhere. A *His2AvD-mRFP* insertion on chromosome III was recombined meiotically with either the *G147* or the *Spider* gene trap insertion and crossed into the pim^1, thr^1 or pim^1 dup^{a1} mutant background.

In vivo imaging

Eggs were collected on apple juice agar plates and aged to the desired stages. Embryos were dechorionated, aligned and immobilized on coverslips according to standard procedures. After covering embryos with halocarbon oil, confocal laser scanning microscopy on an inverted Leica DM IRBE microscope equipped with a TCS SP1 system was used for time-lapse imaging of GFP and mRFP1 fluorescence signals at 22-24°C in a temperature-controlled room. Light damage was prevented by minimizing the laser intensity and opening the pinhole. Frames were acquired at intervals of 10 or 30 seconds. Representative examples of time-lapse movies are provided as supplementary material.

Immunolabeling

Embryos aged to the desired developmental stages were fixed according to standard procedures. For immunofluorescent staining we used mouse anti-γ-tubulin GTU-88 (Sigma) at 1:500, rabbit anti-Bazooka (kindly provided by E. Knust, University of Düsseldorf, Germany) at 1:600, rabbit anti-phospho-histone H3 (Upstate) at 1:800, mouse anti-α-spectrin 9A (Dubreuil et al., 1987) at 1:50, rabbit anti-cyclin B (Jacobs et al., 1998) at 1:2000 and mouse (Promega) and rabbit (Cappel) anti-β-galactosidase at 1:250 and 1:1000, respectively. In addition, secondary goat antibodies conjugated to Alexa488 (Molecular Probes), Cy3 or Cy5 (Jackson Immuno Research Laboratories) were applied. DNA was labeled with either Hoechst 33258 (1 μg/ml) or propidium iodide (1 μg/ml) for confocal microscopy. Terminal transferase dUTP nicked-end labeling (TUNEL) assays of apoptotic cells was performed essentially as described previously (Wang et al., 1999). For comparisons of the density of nucleated cells and of the numbers of mitotic cells, we analyzed three and ten pairs of fixed mutant and sibling wild-type embryos, respectively, which were carefully matched with regard to developmental stage and orientation. Fields of identical size from identical regions of the epidermal cell layer were imaged with a 63× objective and used for the determination of cell and nuclear counts.

Results

Mitosis 16 but not mitosis 15 is severely prolonged in *pim* mutants

The *Drosophila* securin PIM not only functions as an inhibitor of SSE, it also provides a positive function which is absolutely required for sister chromatid separation during mitosis (Stratmann and Lehner, 1996). Nevertheless, initial development of embryos homozygous for pim^1 is normal as long as the maternal pim^+ contribution to the egg provided by the heterozygous mothers is sufficient. However, starting with mitosis 15, this maternal contribution is no longer sufficient for successful divisions. Sister chromatids are therefore not separated during mitosis 15 in pim^1 mutants (Stratmann and Lehner, 1996). The mutation present in pim^1 affects a splice junction (Stratmann and Lehner, 1996) and we have failed to detect protein products expressed from this allele in immunoblotting experiments (data not shown). To complement our previous characterization of fixed embryos by live analyses, we collected eggs from a pim^1/CyO stock carrying two transgenes that result in expression of a red fluorescent histone H2AvD variant (*His2AvD-mRFP*) and a green fluorescent microtubule binding protein. Progression through mitosis 15 in both pim^1 and pim^+ sibling embryos was followed by time-lapse imaging of live embryos. Representative movies from these and the following analyses are available as supplementary material.

As expected from the previous findings with fixed *pim*

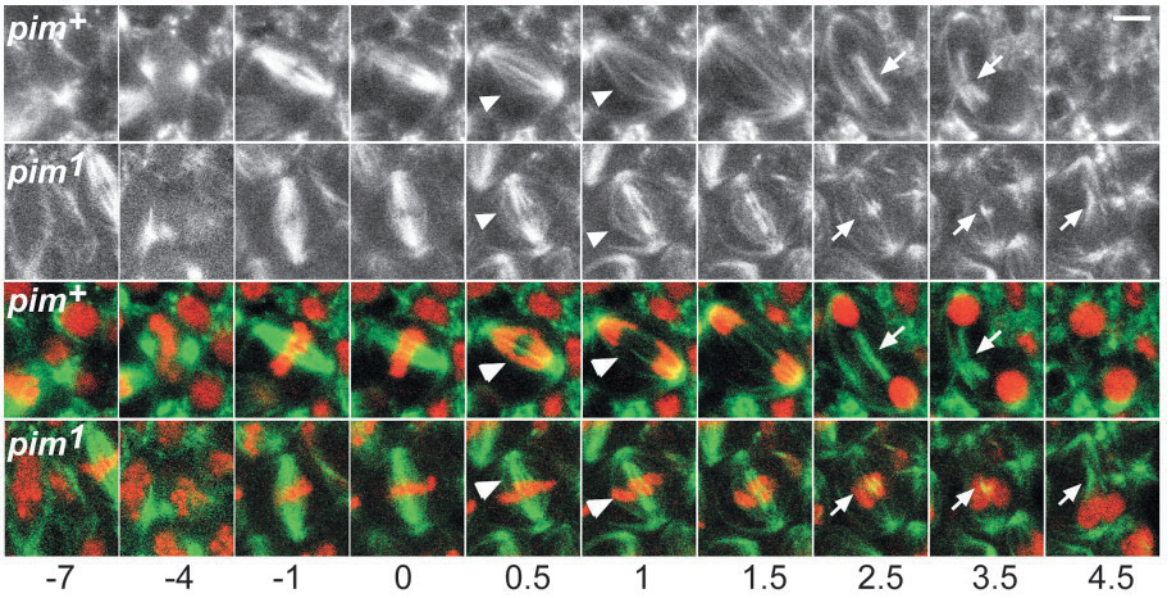

Fig. 1. Exit from mitosis 15 after failure of sister chromatid separation in *pim* mutant embryos. Time-lapse in vivo imaging was used for the analysis of progression through the fifteenth round of mitosis during *Drosophila* embryogenesis in pim^1 mutant (pim^1) and pim^+ (pim^+) sibling embryos expressing red fluorescent histone H2AvD-mRFP and a green fluorescent microtubule-binding protein. Selected frames showing microtubule distribution (top) or merged color images (bottom) are shown. Numbers below the frames indicate the time in minutes relative to the last metaphase frame, which was set to zero. The appearance of prominent interpolar microtubules characteristic of anaphase is indicated by arrowheads. Central spindle and midbody during telophase are indicated by arrows. Bar in upper right frame, 5 μm.

embryos, the first mitotic defects became apparent at the metaphase-to-anaphase transition (Fig. 1). Sister chromatids did not separate in pim^1 mutants. However, the dynamic reorganization of the mitotic spindle that accompanies wild-type anaphase and telophase clearly occurred in pim^1 mutants. The observed spindle behavior in pim^1 mutants during exit from mitosis suggested that absence of separase activity does not have a prominent effect on microtubule stability, in contrast to the findings in budding yeast.

Since budding yeast separase accelerates the exit from mitosis significantly, we compared the speed of chromosome decondensation and spindle disassembly in pim^1 and pim^+ sibling embryos. These comparisons revealed only a minor delay during exit from mitosis in pim^1 mutants (Fig. 1). The time from anaphase onset until the end of mitosis was determined as 4.8 minutes in pim^1 mutant cells (n=10), a value that was only 1.2-fold higher than in the pim^+ sibling embryos (n=7). In vivo imaging using *His2AvD-mRFP* in combination with a GFP fusion protein marking the cell cortex confirmed that progression through mitosis 15 occurs at normal speed in pim^1 mutants except for the surprisingly minor delay during exit from mitosis (Table 1).

Table 1. Dynamics of progression through mitosis in *pim* and *thr* mutants

			Duration (minutes±s.d.)			
Genotype*	Stage†	n‡	Total§	Prophase and metaphase¶	Meta/ana until onset cytokinesis**	Cytokinesis††
pim^+	M15	36	10.0±2.4	6.4±2.2	1.7±0.4	1.8±0.4
pim^1	M15	36	9.9±1.5	6.1±1.2	1.5±0.5	2.4±0.6
thr^1	M15	10	9.6±0.7	5.2±1.0	1.4±0.3	3.0±0.5
pim^+	M16	20	7.4±0.7	4.2±0.6	1.6±0.3	1.6±0.5
pim^1	M16	23	24.2±5.2‡‡	21.5±5.1‡‡	1.4±1.0	3.2±0.9
pim^1 dup^{a1}	M16	32	18.8±5.2	11.7±4.6	2.2±0.7	3.9±1.5
thr^1	M16	10	24.7±7.4‡‡	21.4±7.5‡‡	2.3±0.9	4.75±0.6

*Eggs from parents heterozygous for pim^1, thr^1 or pim^1 dup^{a1}, which also carried a *His2AvD-mRFP* transgene and a gene trap insertion resulting in expression of a GFP fusion protein marking the cell cortex, were collected and used for time-lapse analysis. Homozygous mutant embryos were identified on the basis of the sister chromatid separation failure. pim^+ are sibling embryos without sister chromatid separation failure.

†Progression through mitosis 15 (M15) or mitosis 16 (M16) was analyzed.

‡n=number of mitotic cells analyzed. These mitotic cells were from at least two different embryos.

§Time from the onset of chromosome condensation until completion of cytokinesis.

¶Time from the onset of chromosome condensation until end of metaphase.

**Time from the metaphase-to-anaphase transition (meta/ana, i.e. last metaphase frame) until the onset of cytokinesis (i.e. the first frame in which an equatorial constriction of the cortex was clearly apparent).

††Time from the onset until completion of cytokinesis (i.e. the time from onset until completion of the equatorial constriction of the cell cortex).

‡‡Because almost half of the mitotic cells did not complete mitosis within the analyzed period the given values indicate a minimal and not the actual duration.

Journal of Cell Science

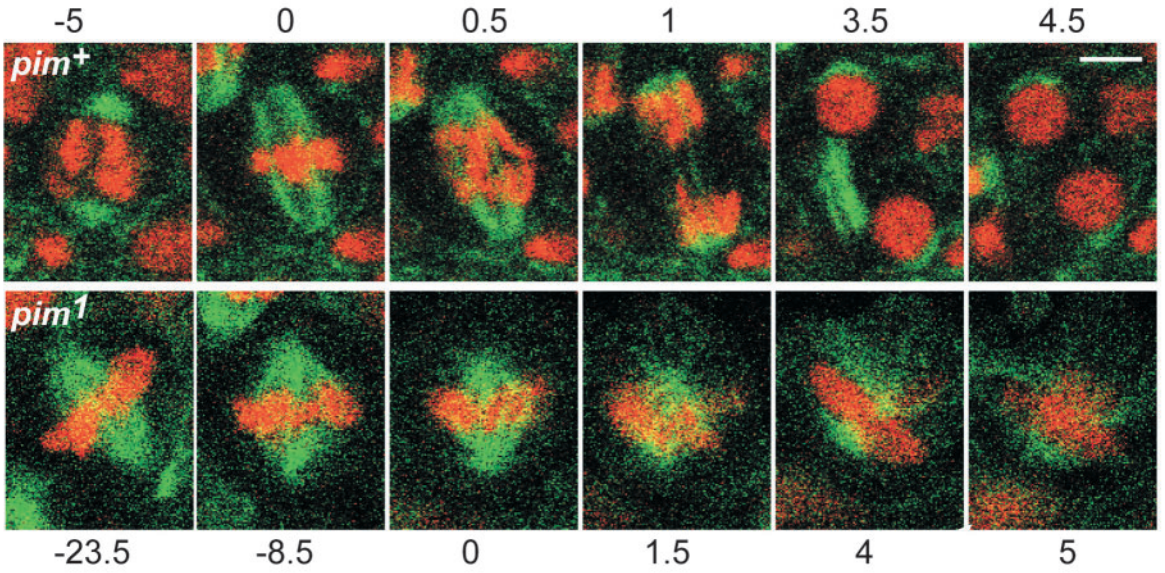

Fig. 2. Metaphase delay during mitosis 16 in *pim* mutant embryos. Time-lapse in vivo imaging was used for the analysis of progression through the sixteenth round of mitosis during *Drosophila* embryogenesis in pim^1 mutant (pim^1) and pim^+ (pim^+) sibling embryos expressing red fluorescent histone H2AvD-mRFP and a green fluorescent microtubule-binding protein. Selected frames of merged images are shown. Numbers above and below the frames indicate the time in minutes relative to the last metaphase frame which was set to zero. Bar in upper right frame, 5 μm.

Diplochromosomes delay the metaphase-to-anaphase transition

After exit from mitosis 15, pim^1 mutants progressed through interphase 16 and entered mitosis 16 without apparent delays. However, during mitosis 16, we observed an extensive delay in the mutants both by in vivo imaging (Fig. 2, Table 1) and in fixed embryos (Fig. 3) where the mitotic index was found to be drastically increased. In pim^1 mutants, mitosis 16 lasts on average at least four times longer than in pim^+ siblings. Therefore in pim^1 mutants mitosis 16 is substantially prolonged in contrast to mitosis 15, which is only slightly delayed.

We considered two potential explanations for the pronounced difference in the dynamics of mitosis 15 and 16 in *pim* mutants. In principle, the difference might reflect the dynamics of the exhaustion of the maternal pim^+ contribution. The levels of residual maternally derived pim^+ function during mitosis 15 might be higher than during mitosis 16. Alternatively, the unusual diplochromosomes, which are present during mitosis 16 in *pim* mutants as a consequence of the sister chromatid separation failure during the preceding mitosis 15 (Stratmann and Lehner, 1996), might trigger the mitotic spindle checkpoint because of difficulties in integrating these abnormal chromosomes in a regular bipolar manner into the mitotic spindle. In this latter case, the delay is expected to occur before the onset of cyclin B degradation which is known to be blocked by the mitotic spindle

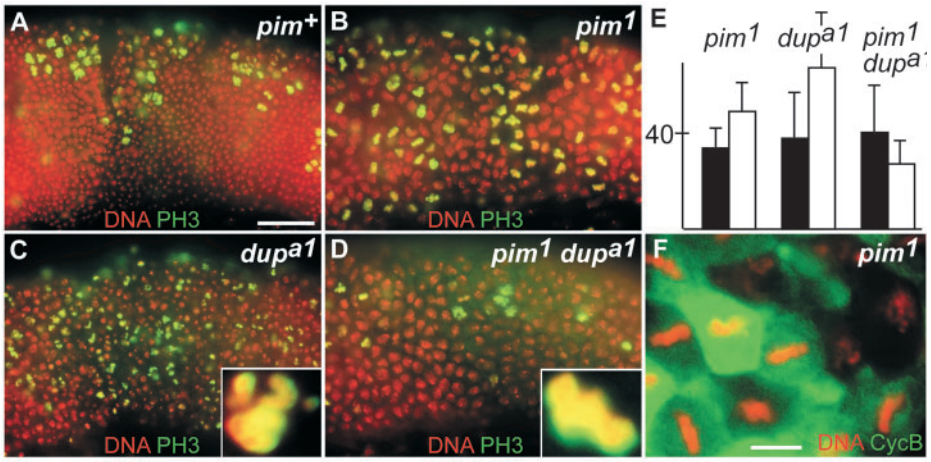

Fig. 3. Metaphase delay during mitosis 16 in *pim* mutants is caused by diplochromosomes. (A-E) Embryos were labeled with a DNA stain (red) and anti-phospho-histone H3 (PH3, green) at the stage of mitosis 16. (A-D) The number of PH3-positive mitotic cells in a defined epidermal region was counted in 10 embryos homozygous for pim^1 (B), dup^{a1} (C), double mutant for both pim^1 and dup^{a1} (D), as well as in pim^+ embryos (A). The resulting average number of mitotic cells (E) in the mutant and the corresponding sibling embryos are indicated by white and black bars, respectively. *dup* encodes an initiation factor for DNA replication; dup^{a1} homozygosity inhibits S phase 16 (Whittaker et al., 2000), as well as the accumulation of mitotic figures in pim^1 mutants during the subsequent mitosis (see text for further explanations). In metaphase cells with maximal PH3 labeling, chromosomes were arranged in metaphase plates in pim^1 dup^{a1} double mutants (inset in D). In contrast, the single chromatid chromosomes present in dup^{a1} mutants failed to congress into a plate (inset in C), as previously described (Parry et al., 2003). Bar, 25 μm (A-D). (F) Labeling with anti-cyclin B (green) and a DNA stain (red) demonstrates that progression through mitosis 16 is delayed before cyclin B degradation in pim^1 mutants. Bar, 10 μm.

Journal of Cell Science

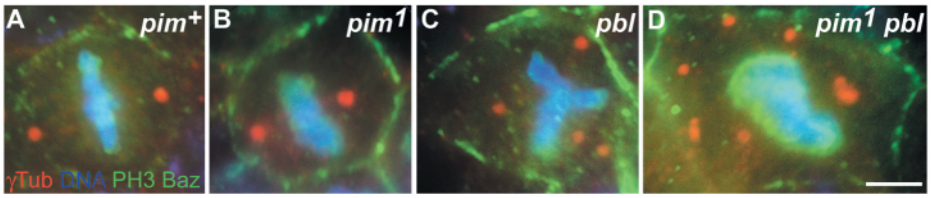

Fig. 4. Centrosome numbers in *pim* mutants. Embryos were labeled at the stage of mitosis 16 (A,B,D) or mitosis 15 (C) with a DNA stain (blue), with anti-phospho-histone H3 (PH3, green) to identify mitotic cells, with anti-Bazooka (Baz, green) to define cell boundaries, and with anti-γ-tubulin (red, γTub) to reveal centrosomes. Maximal projections of representative cells from a pim^{1} mutant (B, pim^{1}), a *pbl* mutant (C, *pbl*), a $pim^{1}pbl$ double mutant (D, pim^{1} *pbl*) and a sibling pim^{+} embryo (A, pim^{+}) are shown, indicating that centrosomes are duplicated in pim^{1} mutants during cycle 16 when cytokinesis during mitosis 15 is inhibited by homozygosity for *pbl* (see text for further explanations). Bar, 3 μm.

checkpoint (Minshull et al., 1989; Whitfield et al., 1990; Minshull et al., 1994). In the former case, however, the delay is not expected to occur before cyclin B degradation because separase is thought to exert its functions only after cyclin B and securin degradation. Immunolabeling of *pim* mutant embryos fixed at the stage of mitosis 16 clearly revealed that the great majority of mitotic cells still contained high levels of cyclin B (Fig. 3F). Moreover, in vivo imaging confirmed that the delay occurred during metaphase, clearly before the onset of anaphase (Fig. 2).

To test whether the abnormal diplochromosomes are responsible for the delay during metaphase of mitosis 16 in *pim* mutants, we analyzed embryos with mutations in both the *pim* and the *double-parked* (*dup*) gene. *dup* encodes the *Drosophila* Cdt1 homolog and is required for DNA replication (Whittaker et al., 2000). As in *pim* mutants, a dup^{+} maternal contribution supports normal initial development. However, dup^{a1} mutant embryos are unable to replicate chromosomes during cycle 16 (Garner et al., 2001; Whittaker et al., 2000). pim^{1} dup^{a1} double mutant embryos therefore should not contain diplochromosomes at mitosis 16 and thus, if the mitotic delay in *pim* single mutants results from the presence of these abnormal chromosomes, it should not occur in the double mutants. Therefore, we analyzed the number of mitotic cells present at the stage of mitosis 16 in pim^{1} and dup^{a1} single and pim^{1} dup^{a1} double mutants. Compared to sibling control embryos (Fig. 3A,E), the number of mitotic cells was not only increased in pim^{1} mutants (Fig. 3B,E) but also in dup^{a1} mutants (Fig. 3C,E). The increased mitotic index in dup^{a1} mutants has previously been described and shown to result from the presence of single chromatid chromosomes, which cannot be stably integrated in a bipolar fashion into the mitotic spindle (Parry et al., 2003; Whittaker et al., 2000). The chromosomes therefore fail to congress into a metaphase plate during mitosis 16 in dup^{a1} mutants (Fig. 3C, inset) (Parry et al., 2003). Moreover, chromosomes are not exposed to tension within the centromeric region and therefore the mitotic spindle checkpoint remains active (Garner et al., 2001; Whittaker et al., 2000). In contrast to pim^{1} and dup^{a1} single mutants, we did not observe an increased number of mitotic cells in the pim^{1} dup^{a1} double mutants (Fig. 3D,E). In addition, chromosomes were found to congress into a metaphase plate (Fig. 3D, inset). These findings, therefore, indicate that the abnormal diplochromosomes are largely responsible for the delay observed during mitosis 16 in the pim^{1} single mutants. This conclusion was fully confirmed by in vivo imaging of the progression through mitosis 16 in pim^{1} dup^{a1} double mutants (Table 1).

The dynamics of mitosis is indistinguishable in *pim* and *thr* mutants

The protein encoded by the *thr* gene corresponds to the N-terminal regulatory domain of separase proteins of other eukaryotes (Jäger et al., 2001; Jäger et al., 2004). The maternal thr^{+} contribution present in thr^{1} mutants is sufficient for normal initial development until mitosis 15. However, just as in *pim* mutants, sister chromatid separation during mitosis 15 fails in thr^{1} mutants (D'Andrea et al., 1993). With our antibodies raised against the C-terminal third of THR, we were unable to detect protein products expressed from the thr^{1} allele, indicating that the mutant protein is either unstable or C-terminally truncated (data not shown). By in vivo imaging we analyzed whether the thr^{1} mutation affects the dynamics of exit from mitosis. However, as observed in the pim^{1} mutants, we detected only a slight delay during exit from mitosis 15 and 16 (Table 1). In addition, we also observed an extensive delay during metaphase 16 (Table 1). To date, neither in vivo imaging nor other analyses have revealed phenotypic differences in pim^{1} and thr^{1} mutants.

pim and *thr* are not required for centrosome duplication and cytokinesis

Our previous phenotypic characterizations of fixed *pim* and *thr* mutant embryos had suggested that cytokinesis during mitosis 15 is not completed in these mutants (D'Andrea et al., 1993; Stratmann and Lehner, 1996). Cleavage furrows pinching the undivided chromosomes were often observed in fixed mutant embryos at the stage of mitosis 15. However, at a later stage, during the following interphase 16, the nuclear density in the epidermal cell layer of fixed mutant embryos was found to be 1.6-fold lower than in sibling control embryos (D'Andrea et al., 1993; Stratmann and Lehner, 1996) (see below), suggesting that the cleavage furrows had failed to cut completely through the chromosomes during mitosis 15. The cleavage furrows were thus thought to have had aborted in most cells.

After such an inferred cytokinesis failure during mitosis 15 and subsequent duplication of centrosomes during cycle 16, mitotic spindles would be predicted to be tetrapolar during mitosis 16 in pim^{1} or thr^{1} mutant cells. In contrast to this expectation, we observed apparently bipolar mitotic spindles and normal metaphase plates during mitosis 16 in pim^{1} and thr^{1} mutants (Fig. 3F, and data not shown). Immunolabeling of centrosomal γ-tubulin demonstrated that the majority of the epidermal cells in pim^{1} and thr^{1} mutant embryos have only two and not four centrosomes at the stage of mitosis 16 (Fig. 4).

In contrast to pim^{1} and thr^{1} mutant embryos, in *pebble* (*pbl*)

Journal of Cell Science

Table 2. Centrosome number in *pim*, *thr* and *pbl* mutants

Genotype*	Stage†	*n*‡	Centrosome number/cell	
			2 or less (%)	More than 2 (%)
pim^{+}	M15	49	100	0
	M16	101	100	0
pim^{1}	M15	51	100	0
	M16	204	85	15
thr^{1}	M15	94	100	0
	M16	282	85	15
pbl^{7O}	M14	85	98	2
	M15	48	10	90
pbl^{11D}	M15	92	5	95
pbl^{+}	M15	89	100	0

*Embryos homozygous for either *pim*^{1}, *thr*^{1}, *pbl*^{7O}, or *pbl*^{11D} were identified by collecting eggs form heterozygous parents with blue balancer chromosomes and scoring for absence of *lacZ* expression. *pim*$^{+}$ and *pbl*$^{+}$ embryos represent *lacZ*-expressing sibling embryos.

†Embryos were aged to the stage of mitosis 14, 15 or 16 (M14, M15 or M16, respectively) before fixation and immunolabeling.

‡*n*=number of mitotic cells analyzed.

mutants the centrosome number was found to increase to four during the cycle following a cytokinesis failure (Fig. 4, Table 2). *pbl* encodes a Rho-GEF required for cytokinesis (Hime and Saint, 1992; Lehner, 1992; Prokopenko et al., 1999). This apparent difference in centrosome behavior in *pim*^{1} and *thr*^{1} mutants, on the one hand, and *pbl* mutants, on the other, raised the question of whether the *Drosophila* separase complex might be required during mitosis for centrosome duplication in the following cell cycle. However, in *pim pbl* double mutants, centrosome number per cell was found to increase with each cycle (Fig. 4), indicating that centrosome duplication is not dependent on the function of the separase complex.

The observed behavior of centrosomes in *pim*^{1} and *thr*^{1} mutants would be readily explained, if these mutations did not interfere with completion of cytokinesis during mitosis 15. Therefore, we re-evaluated cytokinesis in *pim* mutants, this time by in vivo imaging of embryos expressing a green fluorescent cell cortex marker in addition to *His2AvD-mRFP*. Time-lapse recordings clearly demonstrated that cytokinesis is completed successfully during mitosis 15 in the great majority of the epidermal cells in both *pim*^{1} and *thr*^{1} mutants (Fig. 5, and data not shown). The dynamics of cytokinesis was only slightly slower in the mutants compared to sibling controls (Fig. 5, Table 1). The mass of non-separated chromosomes therefore is not a significant obstacle for cytokinesis. In about half of the cells, the cleavage furrow was observed to cut through the chromatin mass, resulting in two daughter cells, which frequently contained unequal amounts of chromatin. In the other half of the cells, the chromatin mass moved towards one pole and cleavage resulted in an enucleate and a nucleate cell pair. Cleavage furrows were not observed to revert after mitosis 15 even during extended observation periods. During the following mitosis 16 in *pim*^{1} and *thr*^{1} mutants, cytokinesis was considerably more abnormal and variable from cell to cell (data not shown). Cleavage furrows were rarely observed to cut through the chromatin mass and they appeared to revert occasionally.

Progression through mitosis without separase function results in epithelial pseudostratification

Our finding that cytokinesis is completed successfully in *pim*^{1} and *thr*^{1} mutants, at least during mitosis 15, was a surprise in the light of the significantly lower densities of cells and nuclei within the superficial epidermal layer in these mutants during cycle 16. Based on our analysis of cytokinesis during mitosis 15, cell density before mitosis 16 should be comparable in *pim*^{1} and *pim*$^{+}$ sibling embryos and the nuclear density should be 25% lower in the mutants. However, cell and nuclear densities were significantly below these expectations. Quantification of the nuclear densities revealed a 38% reduction in *pim*^{1} before mitosis 16. A comparable extensive decrease in the density of nucleated cells was also observed in *thr*^{1} mutant embryos.

In principle, this more extensive reduction might result from apoptosis of the aneuploid cells generated by cytokinesis despite sister chromatid separation failure in *pim*^{1} and *thr*^{1} mutants. To compare the rate of apoptosis in *pim*^{1} and *pim*$^{+}$ sibling embryos we used the TUNEL assay, which detects nucleate apoptotic cells. We did not observe any difference in apoptosis between *pim*^{1} and *pim*$^{+}$ sibling embryos until after the stage of mitosis 16. Up to mitosis 16, we observed only very few apoptotic cells, in the characteristic developmental pattern of programmed cell death in both *pim*^{1} and *pim*$^{+}$ sibling embryos (Fig. 6A,B). After mitosis 16, during germband retraction, *pim*^{1} embryos had slightly more apoptotic cells in regions where developmentally programmed cell death in wild-type is very rare (Fig. 6C,D). After full germband retraction, the number of TUNEL-positive cells was clearly, but still not dramatically, increased in *pim*^{1} mutants (data not shown). Aneuploid cells in *pim* mutants therefore appear to undergo apoptosis eventually, but only after mitosis 16.

To quantify the cellular and nuclear densities in *pim* mutants

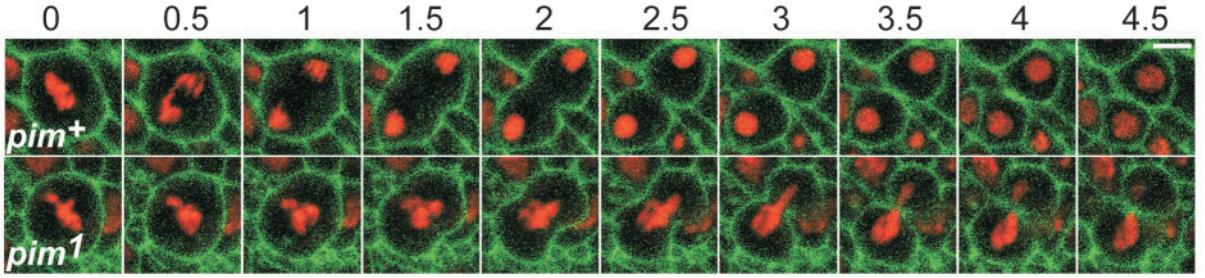

Fig. 5. Cytokinesis during mitosis 15 in *pim* mutants. Time-lapse in vivo imaging was used for the analysis of cytokinesis during the fifteenth round of mitosis during *Drosophila* embryogenesis in *pim*^{1} mutant (*pim*^{1}) and *pim*$^{+}$ (*pim*$^{+}$) sibling embryos expressing red fluorescent histone H2AvD-mRFP and a green fluorescent fusion protein marking the cell cortex. Selected frames of merged images are shown. Numbers above the frames indicate the time in minutes relative to the last metaphase frame which was set to zero. Bar in upper right frame, 5 μm.

Journal of Cell Science

Journal of Cell Science

after mitosis 15, our initial attempts involved double labeling with a DNA stain and an antibody against the apical junction protein Bazooka (BAZ). In *pim*$^{+}$ sibling embryos, each cell displayed an apical ring of anti-BAZ above a centrally located nucleus, as expected. However, in *pim*^{1} mutants, nuclei were very frequently displaced relative to the apical ring of anti-BAZ staining, indicating that the cylindrical organization of the wild-type epithelial cells had been lost (data not shown). Double labeling of DNA and the cell cortex protein α-spectrin further confirmed that the epithelial organization in *pim*^{1} mutants had an abnormal pseudostratified appearance after mitosis 15 but not before (Fig. 7). While single confocal sections through the nucleus of every epidermal cell could readily be obtained in *pim*$^{+}$ sibling embryos before mitosis 16 (Fig. 7C), there were striking irregularities in the sections of *pim*^{1} mutants and they never included all of the nuclei of the nucleated epidermal cells present in other planes of the z stacks (Fig. 7D).

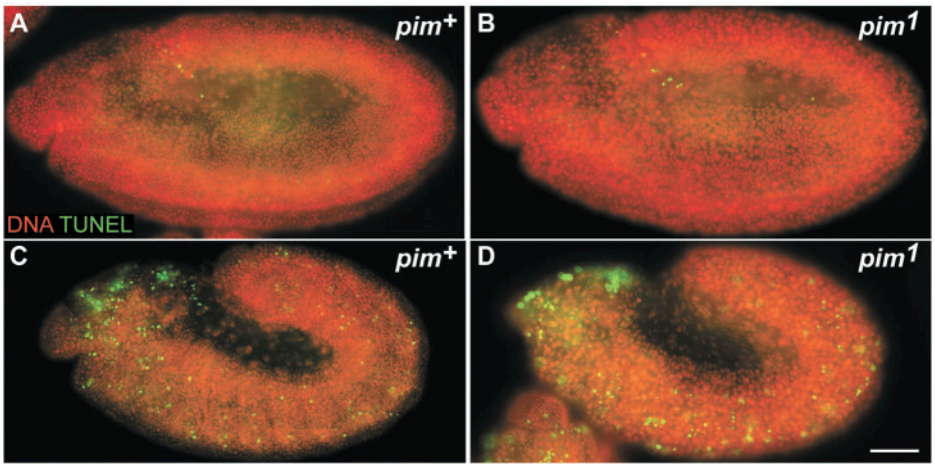

Fig. 6. Apoptosis in *pim* mutants. Embryos before (A,B) or after (C,D) progression through mitosis 16 in the dorsolateral epidermis were labeled with a DNA stain (red) and analyzed by TUNEL (green) for the presence of apoptotic cells. *pim*^{1} mutant embryos (B,D) do not have more apoptotic cells than the *pim*$^{+}$ sibling embryos (A,C), at least before mitosis 16. Bar, 50 μm.

Discussion

To address whether *Drosophila* separase complex subunits provide functions beyond sister chromatid separation during mitosis, we have further characterized the phenotypic consequences of mutations in *pim* and *thr*, which encode the *Drosophila* securin and the equivalent of the N-terminal regulatory domain of non-dipteran separases, respectively.

Our time-lapse analyses of live embryos demonstrate that progression through mitosis 15, i.e. the first mitosis during which the maternal contribution is no longer sufficient for sister chromatid separation in the *pim* and *thr* mutants, is only marginally delayed. The duration of pro- and metaphase 15 did not appear to be affected and the time from anaphase onset until the start of cytokinesis was also not prolonged in the mutants. In contrast, completion of cytokinesis was slightly but significantly extended. This extension by about 1 minute in the *Drosophila* mutants is less than the 20-30 minutes delay during exit from mitosis that results from mutations in the *ESP1* separase gene in budding yeast (Stegmeier et al., 2002; Sullivan and Uhlmann, 2003). The difference in the extent of mitotic delays apparent in *Drosophila* and budding yeast is reduced but not eliminated when expressed relative to the overall duration of exit from mitosis, which lasts about eight times longer in budding yeast.

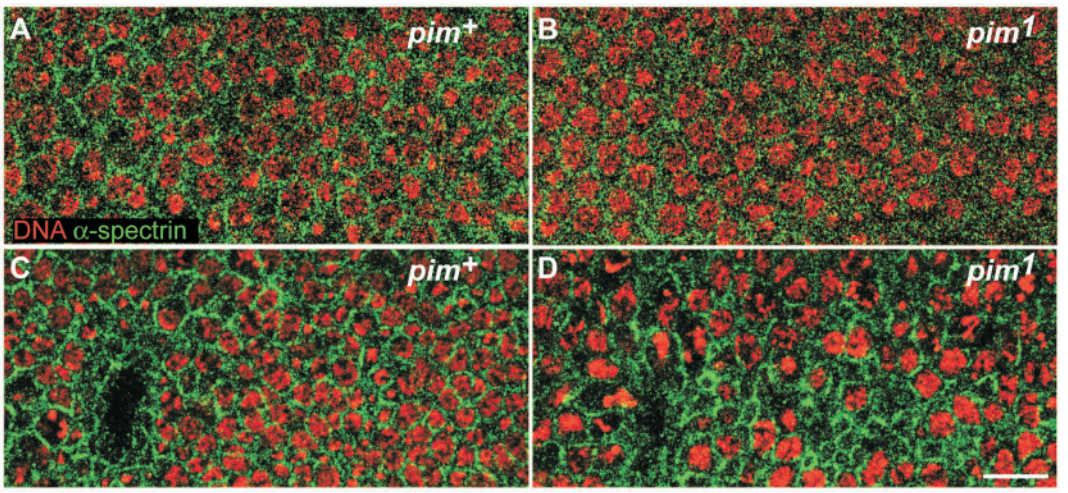

Fig. 7. Epithelial organization in *pim* mutants. Embryos before mitosis 15 (A,B) or before mitosis 16 (C,D) were labeled with a DNA stain (red) and anti-α-spectrin (green). Single confocal sections through the nuclear layer of the epidermal epithelium do not reveal differences between *pim*^{1} mutant (B,D) and *pim*$^{+}$ sibling embryos (A,C) before mitosis 15 (compare A and B). In contrast, a relatively disorganized epidermal epithelium is observed in *pim*^{1} mutants before mitosis 16 (compare C and D). Bar, 10 μm.

While sister chromatid separation is largely inhibited during mitosis 15 in *pim* and *thr* mutants, one exceptional, apparently normal division could be observed in the hundreds of analyzed cells. Therefore, the maternal *pim*$^{+}$ and *thr*$^{+}$ contributions are unlikely to be completely eliminated in the mutants by the time of mitosis 15. As PIM and THR are degraded during mitosis (Herzig et al., 2002; Leismann and Lehner, 2003; Stratmann and Lehner, 1996) any residual maternal contribution, which is still present during mitosis 15, is expected to be further reduced at the

Journal of Cell Science

stage of mitosis 16. The slightly more extensive delay during cytokinesis and exit from mitosis that is observed in the mutants during mitosis 16 might therefore be taken as an indication that a complete elimination of PIM and THR might result in extensive delay. However, alternative explanations are not excluded. Exit from mitosis 16 might be kinetically abnormal not because of a further depletion of the maternal contribution but because of some indirect consequences of the mitosis 15 defects. Mutant cells appear to exit mitosis 16 after adaptation to a spindle checkpoint arrest resulting from mitosis 15 defects (see below). The adaptation mechanisms are unknown and they might have effects on mitosis exit dynamics, which are absent during normal mitosis 16. Such alternative, potential explanations for the slightly stronger delay during exit from mitosis 16 compared to mitosis 15 underscore the technical difficulties of experimental analysis after complete elimination of PIM and THR. In vertebrate systems, the effect of separase on mitotic exit kinetics has not yet been addressed. In *C. elegans*, elimination of separase to a level insufficient for sister chromatid separation does not significantly delay exit from mitosis in controlled osmotic conditions (Siomos et al., 2001).

Arguably the most striking effect on the dynamics of progression through mitosis observed in *pim* and *thr* mutants, i.e. the extensive delay during metaphase of mitosis 16, results indirectly from the failure of sister chromatid separation during mitosis 15. After replication of these non-separated chromatid pairs during S phase 16, *pim* and *thr* mutant cells enter mitosis 16 with abnormal diplochromosomes (Stratmann and Lehner, 1996). Here we demonstrate, with the help of mutations in *Drosophila* Cdt1/Dup, that inhibition of S phase 16 in *pim* mutants prevents most of the delay during metaphase 16. The metaphase extension observed in *pim* and *thr* mutants might therefore be caused by spindle checkpoint activation predominantly resulting from difficulties with bipolar integration of abnormal diplochromosomes into mitotic spindles. We do not understand why the delay during metaphase 16 is not completely reversed in the *pim dup* double mutants, but the residual delay might again reflect adaptation effects, in this case after incomplete inhibition of progression through the preceding S phase 16 (Garner et el., 2001).

Mutations in budding yeast *ESP1*, which abolish protease activity and prevent sister chromatid separation, do not necessarily eliminate activity in the FEAR pathway (Sullivan and Uhlmann, 2003). Therefore the *Drosophila* separase protein which is still present in *pim* and *thr* mutants (Herzig et al., 2002) might be sufficient, in principle, to activate a putative FEAR pathway. Thereby *Drosophila* separase might prevent more extensive mitotic delays in *pim* and *thr* mutants. However, experiments in budding yeast have demonstrated that relatively minor N-terminal truncations abolish FEAR activity of Esp1 (M. Sullivan and F. Uhlmann, personal communication). It appears unlikely, therefore, that *Drosophila* separase, which corresponds to the C-terminal protease domain of Esp1, should be able to function in a putative homologous FEAR pathway in a monomeric form without its usual complex partner THR, which corresponds to the N-terminal domain of Esp1.

In budding yeast, both the proteolytic and the FEAR activity of Esp1 contribute to spindle stability during anaphase, in part by recruiting the budding yeast INCENP-aurora B complex to the central spindle (Pereira and Schiebel, 2003; Ross and Cohen-Fix, 2004; Sullivan et al., 2001). In *Drosophila*, INCENP and aurora B still transfer to the central spindle in *pim* and *thr* mutants during mitosis 15 (A. Herzig and C.F.L., unpublished). Moreover, in vivo imaging has not revealed severe abnormalities in microtubule organization during exit from mitosis 15. Cytokinesis also proceeded surprisingly normally in *pim* and *thr* mutants. Despite an equatorial mass of undivided chromosomes, cleavage furrows contracted rapidly and completely in the mutants during mitosis 15. Therefore, non-separated equatorial chromosomes appear to affect completion of cytokinesis to a variable extent in different cell types. In *Drosophila* and fission yeast, cleavage furrows are definitely able to cut readily through the chromosomes (Uzawa et al., 1990) (Fig. 5). In contrast, in cultured human cells, eventual regression of the cleavage furrow has been observed after expression of mutant SCC1 versions, which cannot be processed by separase (Hauf et al., 2001).

The effects on cytokinesis and spindle organization in the mutants were more prominent during mitosis 16 compared to mitosis 15. Again, as discussed for the mitotic exit kinetics above, this increase in the severity of observed defects might reflect the progressive depletion of the maternal contributions and/or indirect consequences of earlier defects. A rather stochastic segregation of undivided chromosomes during mitosis 15 might generate phenotypic variability during mitosis 16. The observation that some cells exit mitosis 16 in a manner comparable to mitosis 15, while others are more severely affected, therefore argues for indirect consequences.

An interesting aspect of the *pim* and *thr* mutant phenotype revealed by our analyses concerns epithelial organization. Cellularization during wild-type embryogenesis results in a regular monolayer of cylindrical cells, which is maintained in the epidermis throughout the three postblastoderm division cycles, 14-16. In the mutants, this regular epithelial organization is lost after mitosis 15. The abnormal pseudostratified appearance of the epidermis develops rapidly and long before apoptotic responses. The loss of epithelial organization is therefore unlikely to be a consequence of altered gene expression in the aneuploid cells. Rather the loss of separase complex function might affect epithelial organization via effects on the cytoskeleton. Since budding yeast separase has been shown to regulate microtubule stability, a similar role of the *Drosophila* separase complex remains an attractive explanation. Moreover, after mitosis 15, *pim* and *thr* mutant cells contain very variable amounts of chromatin. They contain either no nuclei or nuclei of variable sizes. Since the nucleus might function as a mechanical element within the cells, its variability might contribute to the epithelial disorganization in the mutants. In addition, even though cleavage furrows are able to cut through the undivided chromosomes quite effectively and central spindles as well as midbodies are formed, it is possible that these latter structures are not fully functional, resulting in an inhibition of the establishment of effective junctional contacts between the newly formed daughter cells. The rounding up of cells on the apical side, which occurs upon entry into mitosis, might provide a force that, in particular, displaces some of the already divided cells towards the basal side. Our phenotypic analyses in *Drosophila* embryos emphasize that a loss of separase function can have consequences that might be difficult to

observe with cultured cells. Loss of separase regulation, as for instance after overexpression of the oncogenic human securin PTTG (Melmed, 2003), might promote tumors, not only by increasing genetic instability but also by effects on tissue organization.

We thank A. Herzig for his help with experiments, X. Morin and A. Debec for providing *Drosophila* strains and E. Knust for antibodies. This work was supported by the Fonds der Deutschen Chemie and by grants from the Deutsche Forschungsgemeinschaft (DFG Le 987/3-1, 3-2, 3-3).

References

Bardin, A. J., Visintin, R. and Amon, A. (2000). A mechanism for coupling exit from mitosis to partitioning of the nucleus. *Cell* **102**, 21-31.

Buonomo, S. B., Clyne, R. K., Fuchs, J., Loidl, J., Uhlmann, F. and Nasmyth, K. (2000). Disjunction of homologous chromosomes in meiosis I depends on proteolytic cleavage of the meiotic cohesin Rec8 by separin. *Cell* **103**, 387-398.

Campbell, R. E., Tour, O., Palmer, A. E., Steinbach, P. A., Baird, G. S., Zacharias, D. A. and Tsien, R. Y. (2002). A monomeric red fluorescent protein. *Proc. Natl. Acad. Sci. USA* **99**, 7877-7882.

Ciosk, R., Zachariae, W., Michaelis, C., Shevchenko, A., Mann, M. and Nasmyth, K. (1998). An ESP1/PDS1 complex regulates loss of sister chromatid cohesion at the metaphase to anaphase transition in yeast. *Cell* **93**, 1067-1076.

Clarkson, M. and Saint, R. (1999). A His2AvDGFP fusion gene complements a lethal His2AvD mutant allele and provides an in vivo marker for Drosophila chromosome behavior. *DNA Cell Biol.* **18**, 457-462.

Cohen-Fix, O., Peters, J. M., Kirschner, M. W. and Koshland, D. (1996). Anaphase initiation in Saccharomyces cerevisiae is controlled by the APC-dependent degradation of the anaphase inhibitor Pds1p. *Genes Dev.* **10**, 3081-3093.

D'Amours, D., Stegmeier, F. and Amon, A. (2004). Cdc14 and condensin control the dissolution of cohesin-independent chromosome linkages at repeated DNA. *Cell* **117**, 455-469.

D'Andrea, R. J., Stratmann, R., Lehner, C. F., John, U. P. and Saint, R. (1993). The *three rows* gene of *Drosophila melanogaster* encodes a novel protein that is required for chromosome disjunction during mitosis. *Mol. Biol. Cell* **4**, 1161-1174.

Dubreuil, R., Byers, T. J., Branton, D., Goldstein, L. S. and Kiehart, D. P. (1987). Drosophilia spectrin. I. Characterization of the purified protein. *J. Cell Biol.* **105**, 2095-2102.

Funabiki, H., Yamano, H., Kumada, K., Nagao, K., Hunt, T. and Yanagida, M. (1996). Cut2 proteolysis required for sister-chromatid separation in fission yeast. *Nature* **381**, 438-441.

Garner, M., van Kreeveld, S. and Su, T. T. (2001). mei-41 and bub1 block mitosis at two distinct steps in response to incomplete DNA replication in Drosophila embryos. *Curr. Biol.* **11**, 1595-1599.

Hauf, S., Waizenegger, I. C. and Peters, J. M. (2001). Cohesin cleavage by separase required for anaphase and cytokinesis in human cells. *Science* **293**, 1320-1323.

Herzig, A., Lehner, C. F. and Heidmann, S. (2002). Proteolytic cleavage of the THR subunit during anaphase limits Drosophila separase function. *Genes Dev.* **16**, 2443-2454.

Hime, G. and Saint, R. (1992). Zygotic expression of the *pebble* locus is required during the postblastoderm mitoses of *Drosophila*. *Development* **114**, 165-171.

Jacobs, H. W., Knoblich, J. A. and Lehner, C. F. (1998). Drosophila Cyclin B3 is required for female fertility and is dispensable for mitosis like Cyclin B. *Genes Dev.* **12**, 3741-3751.

Jäger, H., Herzig, A., Lehner, C. F. and Heidmann, S. (2001). Drosophila separase is required for sister chromatid separation and binds to PIM and THR. *Genes Dev.* **15**, 2572-2584.

Jäger, H., Herzig, B., Herzig, A., Sticht, H., Lehner, C. F. and Heidmann, S. (2004). Structure predictions and interaction studies indicate homology of separase N-terminal regulatory domains and Drosophila THR. *Cell Cycle* **3**, 182-188.

Jaspersen, S. L., Charles, J. F. and Morgan, D. O. (1999). Inhibitory phosphorylation of the APC regulator Hct1 is controlled by the kinase Cdc28 and the phosphatase Cdc14. *Curr. Biol.* **9**, 227-236.

Lehner, C. F. (1992). The *pebble* gene is required for cytokinesis in *Drosophila*. *J. Cell Sci.* **103**, 1021-1030.

Leismann, O. and Lehner, C. F. (2003). Drosophila securin destruction involves a D-box and a KEN-box and promotes anaphase in parallel with Cyclin A degradation. *J. Cell Sci.* **116**, 2453-2460.

Leismann, O., Herzig, A., Heidmann, S. and Lehner, C. F. (2000). Degradation of Drosophila PIM regulates sister chromatid separation during mitosis. *Genes Dev.* **14**, 2192-2205.

Melmed, S. (2003). Mechanisms for pituitary tumorigenesis: the plastic pituitary. *J. Clin. Invest.* **112**, 1603-1618.

Minshull, J., Pines, J., Golsteyn, R., Standart, N., Mackie, S., Colman, A., Blow, J., Ruderman, J. V., Wu, M. and Hunt, T. (1989). The role of cyclin synthesis, modification and destruction in the control of cell division. *J. Cell Sci.* **12**, 77-97.

Minshull, J., Sun, H., Tonks, N. K. and Murray, A. W. (1994). A MAP kinase-dependent spindle assembly checkpoint in Xenopus egg extracts. *Cell* **79**, 475-486.

Morin, X., Daneman, R., Zavortink, M. and Chia, W. (2001). A protein trap strategy to detect GFP-tagged proteins expressed from their endogenous loci in Drosophila. *Proc. Natl. Acad. Sci. USA* **98**, 15050-15055.

Parry, D. H., Hickson, G. R. and O'Farrell, P. H. (2003). Cyclin B destruction triggers changes in kinetochore behavior essential for successful anaphase. *Curr. Biol.* **13**, 647-653.

Pereira, G. and Schiebel, E. (2003). Separase regulates INCENP-Aurora B anaphase spindle function through Cdc14. *Science* **302**, 2120-2124.

Prokopenko, S. N., Brumby, A., O'Keefe, L., Prior, L., He, Y., Saint, R. and Bellen, H. J. (1999). A putative exchange factor for Rho1 GTPase is required for initiation of cytokinesis in Drosophila. *Genes Dev.* **13**, 2301-2314.

Ross, K. E. and Cohen-Fix, O. (2004). A role for the FEAR pathway in nuclear positioning during anaphase. *Dev. Cell* **6**, 729-735.

Shou, W., Seol, J. H., Shevchenko, A., Baskerville, C., Moazed, D., Chen, Z. W., Jang, J., Charbonneau, H. and Deshaies, R. J. (1999). Exit from mitosis is triggered by Tem1-dependent release of the protein phosphatase Cdc14 from nucleolar RENT complex. *Cell* **97**, 233-244.

Siomos, M. F., Badrinath, A., Pasierbek, P., Livingstone, D., White, J., Glotzer, M. and Nasmyth, K. (2001). Separase is required for chromosome segregation during meiosis I in Caenorhabditis elegans. *Curr. Biol.* **11**, 1825-1835.

Stegmeier, F., Visintin, R. and Amon, A. (2002). Separase, polo kinase, the kinetochore protein Slk19, and Spo12 function in a network that controls Cdc14 localization during early anaphase. *Cell* **108**, 207-220.

Stratmann, R. and Lehner, C. F. (1996). Separation of sister chromatids in mitosis requires the Drosophila pimples product, a protein degraded after the metaphase anaphase transition. *Cell* **84**, 25-35.

Sullivan, M. and Uhlmann, F. (2003). A non-proteolytic function of separase links the onset of anaphase to mitotic exit. *Nat. Cell Biol.* **5**, 249-254.

Sullivan, M., Lehane, C. and Uhlmann, F. (2001). Orchestrating anaphase and mitotic exit: separase cleavage and localization of Slk19. *Nat. Cell Biol.* **3**, 771-777.

Sullivan, M., Higuchi, T., Katis, V. L. and Uhlmann, F. (2004). Cdc14 phosphatase induces rDNA condensation and resolves cohesin-independent cohesion during budding yeast anaphase. *Cell* **117**, 471-482.

Tinker-Kulberg, R. L. and Morgan, D. O. (1999). Pds1 and Esp1 control both anaphase and mitotic exit in normal cells and after DNA damage. *Genes Dev.* **13**, 1936-1949.

Uhlmann, F., Lottspeich, F. and Nasmyth, K. (1999). Sister-chromatid separation at anaphase onset is promoted by cleavage of the cohesin subunit Scc1. *Nature* **400**, 37-42.

Uhlmann, F., Wernic, D., Poupart, M. A., Koonin, E. V. and Nasmyth, K. (2000). Cleavage of cohesin by the CD clan protease separin triggers anaphase in yeast. *Cell* **103**, 375-386.

Uzawa, S., Samejima, I., Hirano, T., Tanaka, K. and Yanagida, M. (1990). The fission yeast cut1+ gene regulates spindle pole body duplication and has homology to the budding yeast esp1 gene. *Cell* **62**, 913-925.

Visintin, R., Craig, K., Hwang, E. S., Prinz, S., Tyers, M. and Amon, A. (1998). The phosphatase Cdc14 triggers mitotic exit by reversal of Cdk-dependent phosphorylation. *Mol. Cell* **2**, 709-718.

Waizenegger, I. C., Hauf, S., Meinke, A. and Peters, J. M. (2000). Two distinct pathways remove mammalian cohesin from chromosome arms in prophase and from centromeres in anaphase. *Cell* **103**, 399-410.

Wang, S. L., Hawkins, C. J., Yoo, S. J., Muller, H. A. and Hay, B. A. (1999). The Drosophila caspase inhibitor DIAP1 is essential for cell survival and is negatively regulated by HID. *Cell* **98**, 453-463.

Journal of Cell Science

Whitfield, W. G. F., Gonzalez, C., Maldonado-Codina, G. and Glover, D. M. (1990). The A- and B-type cyclins of Drosophila are accumulated and destroyed in temporally distinct events that define separable phases of the G2-M transition. *EMBO J.* **9**, 2563-2572.

Whittaker, A. J., Royzman, I. and Orr-Weaver, T. L. (2000). Drosophila double parked: a conserved, essential replication protein that colocalizes with the origin recognition complex and links DNA replication with mitosis and the down-regulation of S phase transcripts. *Genes Dev.* **14**, 1765-1776.

Zou, H., McGarry, T. J., Bernal, T. and Kirschner, M. W. (1999). Identification of a vertebrate sister-chromatid separation inhibitor involved in transformation and tumorigenesis. *Science* **285**, 418-422.

Journal of Cell Science